Original Article

Evaluating the stage of deep vein thrombosis: the diagnostic accuracy of shear wave elastography and super-microvascular imaging

Lin Peng[1], Yan Liu[2], Chunju Lv[2], Wenyi Shen[2], Yanqing Wu[3], Jiajun Zhang[2], Zunfeng Fu[2]^

[1]Department of General Practice, The Second Affiliated Hospital of Shandong First Medical University, Tai'an, China; [2]Department of Ultrasound, The Second Affiliated Hospital of Shandong First Medical University, Tai'an, China; [3]Department of Ultrasound, Xintai People's Hospital, Tai'an, China

Contributions: (I) Conception and design: L Peng, Y Liu, Z Fu; (II) Administrative support: J Zhang; (III) Provision of study materials or patients: L Peng, C Lv, W Shen, Y Wu; (IV) Collection and assembly of data: C Lv, W Shen, Y Liu; (V) Data analysis and interpretation: L Peng, J Zhang, Z Fu; (VI) Manuscript writing: All authors; (VII) Final approval of manuscript: All authors.

Correspondence to: Zunfeng Fu, MD. Department of Ultrasound, The Second Affiliated Hospital of Shandong First Medical University, No. 366 Taishan Street, Taishan District, Tai'an 271000, China. Email: fuzunfeng@163.com.

Background: Assessing the age of deep vein thrombosis (DVT) is crucial for guiding treatment approaches. Two-dimensional shear-wave elastography (2D-SWE) and super-microvascular imaging (SMI), as emerging techniques for tissue elasticity assessment and intrathrombus microvascular analysis, are pivotal for accurate thrombus age determination. This research endeavors to classify DVT into acute, subacute, and chronic ages utilizing these imaging methods.

Methods: The study is a prospective, single-center, inpatient investigation that utilized convenience sampling for participant recruitment. Patients with a symptom duration of <6 months who were found to have lower-extremity DVT on ultrasound (US) between January 2021 and March 2022 after craniocerebral trauma (CT) or bone injury (BI) operations were included in this study. Participants were divided into three groups based on the duration of DVT, measured from the first diagnosis of thrombosis by US to the follow-up with 2D-SWE and SMI: acute (≤14 days), subacute (15–30 days), and chronic (31 days to 6 months) All patients underwent 2D-SWE and SMI using an Aplio i700 Ultrasound System equipped with a PLT-1005BT line array probe. Diagnostic performance was assessed using the area under the receiver operating characteristic (ROC) curve.

Results: The maximum value of the elastic modulus for DVT (DVT_Emax), the mean value of the elastic modulus for DVT (DVT_Emean), and SMI's flow distribution scoring pattern for DVT (SMI_scoring) emerged as significant predictors for acute and chronic, with high area under the ROC curve (AUC) of acute [AUC (95% confidential interval): 0.95 (0.89–0.97), 0.96 (0.91–0.98), 0.93 (0.88–0.97) in 39 patients] and chronic [AUC (95% confidential interval): 0.88 (0.81–0.93), 0.94 (0.88–0.97), 0.91 (0.84–0.95) in 51 patients], respectively. However, these indices had lower efficacy for subacute prediction [AUC (95% confidential interval): 0.51 (0.42–0.60), 0.54 (0.46–0.63), 0.53 (0.44–0.62), in 47 patients]. Combining DVT_Emean with SMI_scoring improved performance in predicting subacute: 0.90 (0.83–0.94) than related features alone.

Conclusions: Both 2D-SWE and SMI can be used to assess acute and chronic DVT in patients with CT and BI after surgeries. This combination is a promising adjunctive technique for identifying the subacute phase of DVT in these patients.

^ ORCID: 0000-0003-4872-8183.

Keywords: Deep vein thrombosis (DVT); two-dimensional shear-wave elastography (2D-SWE); super-microvascular imaging (SMI); ultrasound (US)

Submitted Jan 03, 2024. Accepted for publication Apr 22, 2024. Published online May 21, 2024.
doi: 10.21037/qims-23-1822
View this article at: https://dx.doi.org/10.21037/qims-23-1822

Introduction

Deep vein thrombosis (DVT) is a common condition with an incidence of approximately 1 in 1,000 individuals per year (1). DVT typically occurs in the lower extremities, whereas upper-extremity DVT occurs less frequently and is often associated with catheter use. Ultrasound (US) is considered the best noninvasive choice for the diagnosis of DVT and has high sensitivity and specificity for thrombosis involving the proximal veins of the legs, that is, the femoral and popliteal veins (2). In US examinations, the vein diameter, vein compressibility, thrombus echogenicity, and duration of patient complaints are commonly used to differentiate between early and chronic DVT (3-5). However, there is insufficient evidence to confirm that such methods are reliable and replicable tools for assessing thrombus age. Several factors can affect the assessment such as patient ambiguity, not remembering of the time of symptom onset, subjective judgments by US operators, and controversial interpretations of color and two-dimensional US results. Moreover, most patients with postoperative DVT have no specific symptoms, likely because the thrombi are very small (in some cases, 1 cm in length) and often do not cause vein occlusion (6).

Although most cases of postoperative DVT are isolated from the calf veins - isolated distal DVT (ID-DVT), 20–50% may involve the more proximal venous system (7). Recommendations of antithrombotic therapy for venous thromboembolism (8) suggest extension of ID-DVT that would favor anticoagulation over surveillance (e.g., >5 cm in length, involving multiple veins, >7 mm in maximum diameter, detected by US). Timely US surveillance is needed in asymptomatic patients with postoperative DVT; As well, knowing the age of DVT is important for clinical and therapeutic implications. Acute thrombi, which consist mainly of fibrin, are highly sensitive to anticoagulation and thrombolytic therapies; however, chronic thrombi are highly resistant to therapy as fibrinolysis ends. Two-dimensional shear-wave elastography (2D-SWE) and super-microvascular imaging (SMI) may be helpful in assessing DVT age.

Based on shear-wave velocities, the US system provides a quantitative measure of tissue elasticity (9,10). On the US screen, shear modulus maps are represented as a color-coded elastogram displaying shear-wave velocities in meters per second (m/s) or tissue elasticity in kilopascals (kPa) to reflect changes in tissue stiffness. According to a recent meta-analysis (11), despite significant differences in the study design, definitions of thrombus age, and patient characteristics, nearly all studies (9,10,12-14) demonstrated an increase in thrombus stiffness according to DVT age (from acute to chronic). However, there was substantial variation in the definitions of acute, subacute, and chronic DVT, leading to differences in the interpretation of the results and their clinical application.

SMI is a US imaging modality that has been routinely used since 2014 (15). It is based on a unique algorithm that identifies and eliminates clutter while preserving low-flow signals, which enables visualization of microvessels in tumors and carotid plaques. In DVT, after as few as 7 days, acute venous thromboembolism demonstrates elements of organization, including collagen deposits, neovascularization, and increased leukocyte infiltration (16,17). Accordingly, we hypothesized whether the SMI technique could detect neovascularization in the histologic features of the thrombus. However, to date, no studies have used SMI to assess DVT age. Based on our initial pilot observations, we identified that SMI can detect instances of partial neovascularization in DVT that have persisted beyond 14 days. While neovascularization was also observed in a limited number of chronic cases (over 30 days), its occurrence was notably more frequent and specific during the subacute phase (15–30 days). Drawing on the DVT aging methodologies established in prior researches (10) and integrating our own findings, we set out to classify DVT into acute (≤14 days), subacute (15–30 days), and chronic (31 days to 6 months) phases. This approach aimed to provide a more nuanced understanding of the DVT's progression and neovascularization at different ages.

We also limited our study to postoperative populations with craniocerebral trauma (CT) or bone injuries (BI) and

used the interval between two US examinations (one for the first diagnosis of DVT and the other for applying 2D-SWE and SMI) to define DVT aging [postoperative patients, firstly, with surgery and immobilization as DVT risk factors, are often identified with thrombosis during hospital US examinations. This approach precisely establishes the timing of thrombus formation, avoiding inaccuracies from inquiries of patient history (relying on the onset of patients' clinical symptoms). Secondly, these patients' good post-discharge compliance reduces follow-up loss. Thirdly, focusing on these patients also ensures a uniform study population, preventing imaging feature overlap from varied other etiologies]. We present this article in accordance with the STARD reporting checklist (available at https://qims.amegroups.com/article/view/10.21037/qims-23-1822/rc).

Methods

Patients

The study was conducted in accordance with the Declaration of Helsinki (as revised in 2013). The study was approved by Institutional Review Board of The Second Affiliated Hospital of Shandong First Medical University (No. 202047) and informed consent was taken from all individual participants. Between January 2021 and March 2022, a convenience sample of 137 patients (62 males, 75 females) with common femoral vein thrombosis (CFVT), popliteal vein thrombosis (POPVT), combined vein thrombosis (CVT), including both CFVT and POPVT, or extension of ID-DVT (length >5 cm, width >7 mm) diagnosed by compression US were enrolled, and all patients underwent CT or BI surgery. The first recorded time was when routine postoperative US screening detected thrombi. The SWE and SMI operators were unaware of the specific time of thrombus existence; they only knew that the patient had clots (*Figure 1*).

The inclusion criteria for DVT US were as follows: (I) the diagnosis was confirmed by routine postoperative US screening; and (II) all patients underwent lower extremity venous US and the SWE and SMI examinations again to confirm clear thrombus staging. Patients were excluded for the following reasons: (I) history of DVT upon admission (residual adhesions or scars within the venous lumen, which can potentially affect the measurement results of SWE and SMI in the case of recurrent thrombosis); (II) individuals with comorbid psychiatric conditions or dementia impacting their ability to cooperate with the examination; (III) patients with a (distance from the thrombus center to body surface ≥3.0 cm), excessive obesity, or lower-limb edema that significantly affected the measurements and image quality; and (IV) those with systemic infectious diseases or other conditions that may affect thrombus staging.

The enrolled patients were categorized into three groups according to DVT age: acute (39 patients), subacute (47 patients), and chronic (51 patients).

Conventional US, SMI, and 2D-SWE imaging

All US, 2D-SWE and SMI examinations were performed using the same US machine (Canon Aplio i700, PLT-1005BT line array probe, 5–14 MHz) by the same operator (Y.L.), who had 8 years of experience with vascular US and 3 years with 2D-SWE and SMI and was blinded to the clinical history during the examinations. Ultrasonographic images of CFVT were obtained near the junction of the greater saphenous vein, and thrombi were observed in this area. If no clots were present at this level, images were captured at the proximal level of the common femoral vein with clots. To confirm the diagnosis of DVT and determine its extent, we performed compression US from the common iliac vein to the calf veins in both the transverse and longitudinal planes. Color Doppler flow imaging (CDFI), power Doppler imaging, and US SMI were employed to verify the blood flow around the thrombi.

Grayscale US settings were standardized to ensure consistency and reproducibility. Specifically, a dynamic range of 60° was utilized with a gain setting of 86%. The time gain compensation was centered, and the focus position was adjusted to the midpoint of the DVT. To interpret the echogenicity of the thrombus, echoes from the surrounding muscle tissue were used as references. If the thrombus displayed echoes that were lower than those of the surrounding muscle tissue, it was categorized as hypoechoic, scoring 1 point in a semi-quantitative analysis of DVT echogenicity (DVT_echo). If the echoes were similar to the muscle tissue, the thrombus was designated as isoechoic and, assigned a score of 2 points. Conversely, if the echoes were higher than the muscle tissue, the thrombus was classified as hyperechoic, with a score of scoring 3 points.

When the 2D-SWE mode was activated, the transducer was immobilized without any movement or compression, and the 2D-SWE box was adjusted to target DVT. Images were frozen and saved. Three consecutive valid 2D-SWE images were obtained from the same imaging plane for

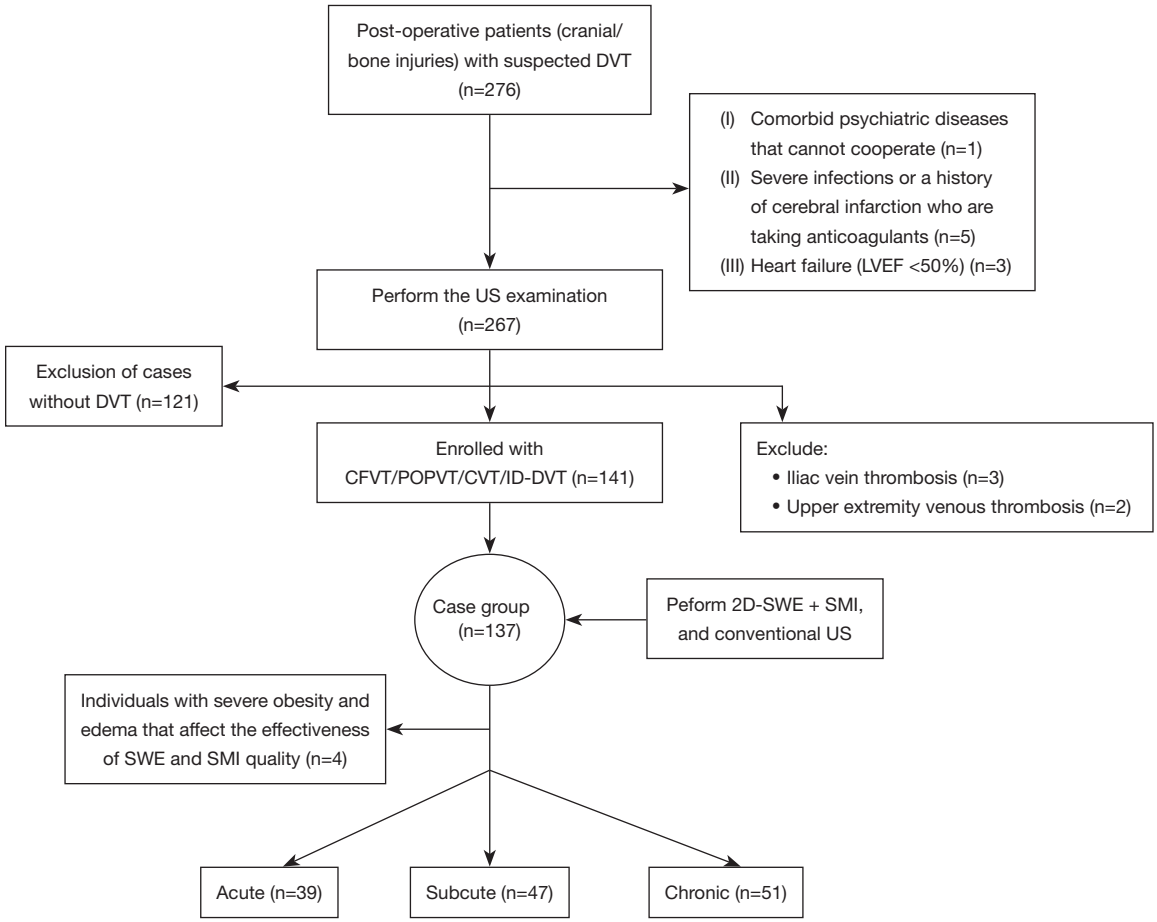

Figure 1 Patient enrollment flowchart. DVT, deep vein thrombosis; LVEF, left ventricular ejection fraction; US, ultrasound; CFVT, common femoral vein thrombosis; POPVT, popliteal vein thrombosis; CVT, combined vein thrombosis; ID-DVT, isolated distal deep venous thrombosis; 2D-SWE,two-dimensional shear wave elastography; SMI, super-microvascular imaging. Acute: ≤14 days; Subacute: 15–30 days; Chronic: 31 days to 6 months.

each patient. If the color-filled area of the elastic image was very small or less than half, detection was considered unsuccessful (18,19).

The size and location of the region of interest (ROI) for 2D-SWE were standardized by (I) avoiding the vessel wall and blood flow surrounding the thrombi by CDFI and SMI; (II) avoiding the proximal floating thrombus tip located at the deep vein; and (III) varying the number (3–10 per image) and site of ROIs for each image depending on the size of the thrombi. If ROIs were applied, they were placed without overlapping. To obtain a representative value of DVT for each acquisition, the peak and average values of three consecutive acquisitions were determined as the ultimate elastic modulus of DVT (DVT_Emax, DVT_Emean).

The SMI's flow distribution scoring pattern (SMI_scoring) was scored using a semi-quantitative system that assigned a score of one if no flow or only surrounding flow was present; two if there was only peripheral flow distribution within the thrombus (perpendicular to the vein wall and spectral Doppler images showing an arterial pattern); three if spectral Doppler showing a venous pattern and the percentage of SMI within the thrombus was ≤50%; and four for thrombi with a >50% SMI area (*Figure 2*).

Variability analysis

Interobserver variabilities for DVT_Emax, DVT_Emean,

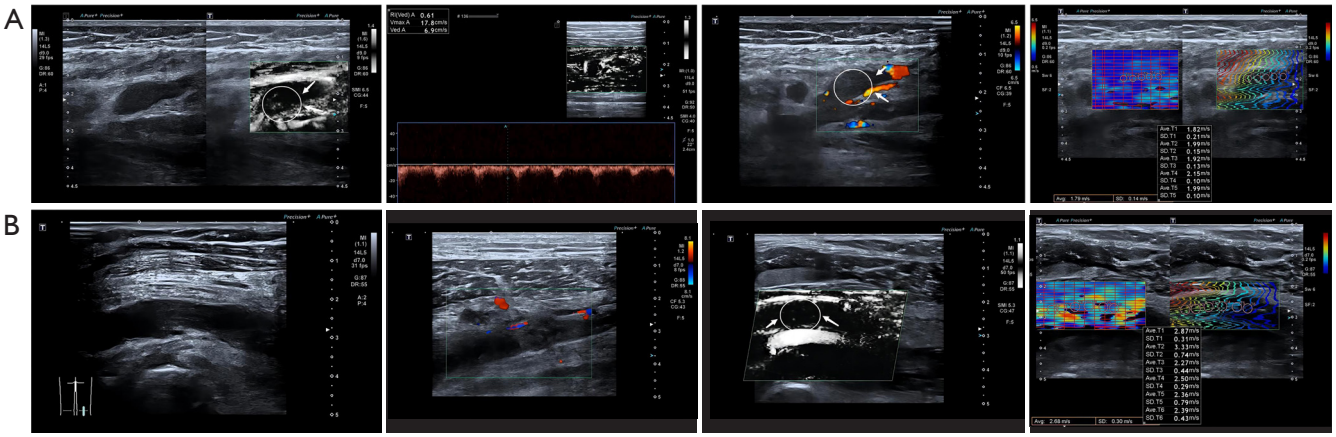

Figure 2 Measurement of DVT using 2D-SWE and SMI. (A) A 16-day subacute ID-DVT image. CDFI depicts only peripheral blood flow surrounding the thrombus (the circles demarcated by arrows illustrate the distribution of blood flow within and surrounding the thrombus by CDFI or SMI); SMI displays neovascularization within the thrombus, scored 2 (long and short axes) and SWE indicates a DVT_Emean of 11.6 kPa and a DVT_Emax of 13.8 kPa, respectively. (B) A 48-day chronic POPVT image. CDFI also shows peripheral blood flow; the SMI area (<50% thrombus) scored 3 with no arterialized spectrum, and SWE suggests a DVT_Emean of 22.1 kPa and a DVT_Emax of 32.4 kPa, respectively. DVT, deep vein thrombosis; 2D-SWE, two-dimensional shear wave elastography; SMI, super microvascular imaging; ID-DVT, isolated distal deep venous thrombosis; CDFI, color doppler flow imaging; SWE, shear wave elastography; DVT_Emean, the mean value of the elastic modulus for DVT; DVT_Emax, the maximum value of the elastic modulus for DVT; POPVT, popliteal vein thrombosis.

SMI_scoring, and DVT_echo were analyzed in 30 random cases. To determine interobserver variability, a second investigator (C.L.), who also had 8 years of experience with vascular US and 3 years with 2D-SWE and SMI and was blinded to the results of the first operator (Y.L.) and clinical data, reanalyzed the measurements.

Statistical methods

Statistical analyses were performed using MedCalc Statistical Software version 20.022 (MedCalc Software Ltd., Ostend, Belgium; https://www.medcalc.org; 2021). The Shapiro-Wilk test was used to assess the normality of continuous variables. These normally distributed variables were assessed using the one-way analysis of variance, followed by Scheffé's post-hoc test. Non-normally distributed variables were expressed as median (interquartile range) and were compared using the Kruskal-Wallis H test, followed by Dunn's post-hoc test. Categorial variables among the three groups were assessed using the chi-squared test or Fisher's exact test. Spearman's coefficient was used to determine the correlation between the DVT stage and test results. The diagnostic efficiencies of SMI, 2D-SWE and their combined model (using binary logistic regression model) were assessed using receiver operating characteristic (ROC) curve and the cut-off values are identified as the points maximizing the Youden's Index, representing the optimal balance between sensitivity and specificity.The area under the ROC curve (AUC) analysis using the following parameters: acute *vs.* subacute-chronic (acute), acute-subacute *vs.* chronic (chronic), and acute-chronic *vs.* subacute (subacute). AUCs were compared using the method proposed by DeLong *et al.* (20). Point estimates and 95% confidence intervals were calculated. Statistical significance was defined as $P<0.05$ for two-tailed tests.

The sample size for this study was estimated based on preliminary results. DVT_Emean was identified as the main indicator using factorial analysis of variance. The test parameters were as follows: $\alpha=0.05$, $1-\beta=0.90$, AUC 0 (0.5), and AUC 1 (0.7–0.97) (6-8). At least 32 participants in each group were required. The sample size and power were calculated using PASS2023, version 23.0.2 for Windows (NCSS, Kaysville, UT, USA).

Results

Comparison of general information

Patients were grouped according to the time of the two US examinations (days): acute, subacute, and chronic. Age,

Table 1 Basic characteristics of the participants

Characteristics	Acute (n=39)	Subacute (n=47)	Chronic (n=51)	F/χ^2	P value
Age (years)	49±16	48±17	49±16	0.37	0.82
Male	18 [46]	24 [51]	20 [39]	1.20	0.55
BMI (kg/m^2)	25.44±3.26	24.89±4.11	24.42±3.74	0.57	0.76
Hypertension	14 [36]	21 [45]	28 [55]	3.26	0.20
Current smoker	11 [28]	12 [26]	22 [43]	3.97	0.14
Diabetes	8 [21]	14 [30]	19 [37]	2.96	0.23
CT patients	11 [28]§	14 [30]§	37 [73]†‡	24.45	<0.0001
DVT position					
CFVT	5 [13]§	8 [17]§	20 [39]†‡	10.3	0.006
POPVT	8 [21]§	11 [23]§	21 [41]†‡	5.73	0.06
Extension of ID-DVT	22 [56]§	20 [43]§	2 [4]†,‡	31.50	<0.001
CVT	4 [10]	8 [17]	8 [16]	0.86	0.65
D-D (mg/L)	3.75 (1.42–8.90)	3.34 (2.40–3.80)	1.80 (0.99–2.77)†‡	15.56	0.03
Anticoagulation treatment	15 [38]‡§	40 [85]†	48 [94]†	46.1	<0.001

Data are presented as mean ± standard deviation, number [percentage], or median (interquartile range). †, P<0.05 *vs.* acute; ‡, P<0.05 *vs.* subacute; §, P<0.05 *vs.* chronic. BMI, body mass index; CT, craniocerebral trauma; DVT, deep venous thrombosis; CFVT, common femoral vein; POPVT, popliteal vein thrombosis; extension of ID-DVT, isolated distal deep venous thrombosis (length >5 cm, width >7 mm); CVT, combined vein thrombosis, including both CFVT and POPVT; D-D, D-dimer.

sex, body mass index (BMI), hypertension, current smoking status, and diabetes were not significantly different between the groups (all P>0.05). No differences were observed between the acute and subacute BI or CT groups. However, there were more patients with CT than BI in the chronic group. Regarding the position of DVT, in both BI and CT patients, ID-DVT was most common in the acute and subacute groups. There was also a difference in D-dimer levels, which were lowest in the chronic group; however, no difference was found between the other groups (*Table 1*).

DVT_echo, 2D-SWE features, and SMI_scoring

Table 2 shows the US characteristics of the patients. There was only a weak positive correlation between DVT_echo and DVT age (ρ=0.49, P<0.001). Strong positive correlations were observed between DVT_Emean, DVT_Emax, SMI_scoring, and DVT age (ρ=0.75, P<0.001; ρ=0.72, P<0.001; ρ=0.82, P<0.001). In addition, there were differences in DVT_Emean, DVT_Emax, and SMI_scoring among the study patients with different DVT ages (P<0.001). There was no statistically significant difference in DVT_echo between the acute and subacute groups (*Table 2*, *Figure 3*).

Diagnostic performance of SMI, DVT_echo, and 2D-SWE features

The diagnostic performance of the US and 2D-SWE features in predicting DVT stages is detailed in *Table 3* and *Figure 4*. For the prediction of acute DVT, DVT_Emax, DVT_Emean and SMI_scoring outperformed DVT_echo and combined model of DVT_Emean and SMI_scoring (using a binary logistic regression model) (all P<0.001), with no significant difference between DVT_echo and the combined model (P=0.98). For prediction of subacute age, only the combined model's AUC was significant (P<0.001), while other parameters showed no significant differences (all P<0.05). For the prediction of chronic age, the AUCs of DVT_Emean and SMI_scoring were higher than those of the other characteristics (all P<0.01).

However, overlap cutoff values were obtained for DVT_Emean (≤19.7 kPa for subacute, and >17.3 kPa for chronic) and DVT_Emax (≤27.4 kPa for subacute, and >20.5 kPa for chronic) in predicting subacute and chronic. Owing to conflicting or nearly equal cutoff values for DVT_Emean, DVT_Emax, and SMI_scoring in predicting subacute and chronic diseases, neither parameter can be

Table 2 Comparison of DVT_Emean, DVT_Emax, SMI_scoring, and DVT_echo, in patients with DVT

Characteristics	Acute (n=39)	Subacute (n=47)	Chronic (n=51)	ρ	H	P
DVT_Emean (kPa)	10.30 (9.10–11.70)[‡§]	15.55 (13.56–17.70)[†§]	21.37 (17.84–28.80)[†‡]	0.75	95.23	<0.001
DVT_Emax (kPa)	14.30 (13.10–15.90)[‡§]	20.20 (18.15–24.34)[†§]	26.67 (22.13–32.29)[†‡]	0.72	84.19	<0.001
SMI_scoring	1.0 (1.0–1.0)[‡§]	2.0 (2.0–3.0)[†§]	3.0 (3.0–4.0)[†‡]	0.82	92.93	<0.001
DVT_echo	1.0 (1.0–1.0)[§]	1.0 (1.0–1.0)[§]	1.0 (1.0–2.0)[†‡]	0.49	38.73	<0.001

Data are presented as median (interquartile range). [†], P<0.05 *vs*. acute; [‡], P<0.05 *vs*. subacute; [§], P<0.05 *vs*. chronic. DVT_Emean, the mean value of the elastic modulus for DVT; DVT_Emax, the maximum value of the elastic modulus for DVT; SMI_scoring, SMI's flow distribution scoring pattern; DVT_echo, deep vein thrombosis echogenicity; DVT, deep vein thrombosis; ρ, Spearson correlation coefficient; SMI, super microvascular imaging.

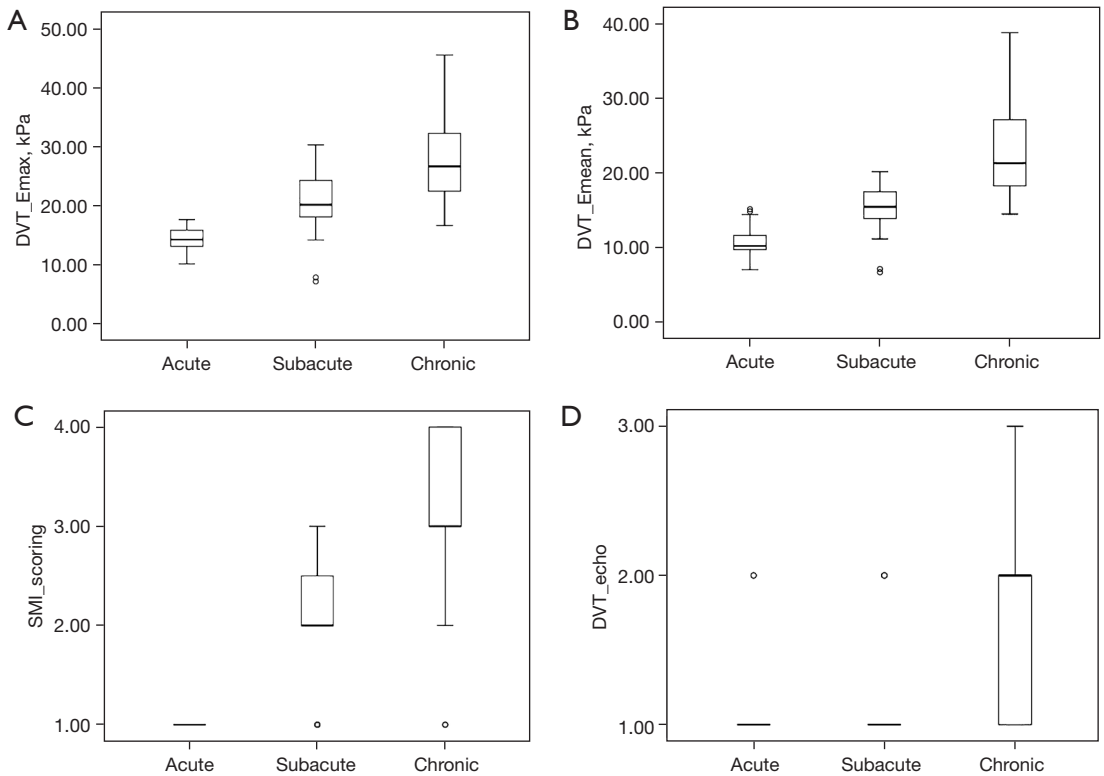

Figure 3 Box and whisker plots of indices in the study population according to DVT age. (A) DVT_Emax. (B) DVT_Emean. (C) SMI_scoring. (D) DVT_echo. The top and bottom of each box are the 75th and 25th percentiles, respectively; the horizontal line in each box is the median (50th percentile); the top and bottom of the whiskers are the minimum and maximum, and "○" represents outlier, respectively. Acute: ≤14 days; Subacute: 15–30 days; Chronic: 31 days to 6 months. DVT_Emax, the maximum value of the elastic modulus for DVT; DVT_Emean, the mean value of the elastic modulus for DVT; SMI_scoring, SMI's flow distribution scoring pattern; DVT_echo, deep vein thrombosis echogenicity; DVT, deep venous thrombosis; SMI, super microvascular imaging.

considered a useful indicator for determining subacute disease. Surprisingly, the combined model demonstrated good diagnostic efficacy for subacute DVT. Its AUC was 0.89, and the sensitivity, specificity, positive predictive value, negative predictive value, and accuracy were 87.23%, 86.67%, 77.36%, 92.85%, and 86.86%, respectively.

Table 3 Optimal cut-off values and areas under ROC curve of parameters for predicting DVT ages

Parameters	Optimal cutoff	AUCs (95% CI)	P† value for comparison of AUCs			
			vs. DVT_Emean	*vs*. DVT_Emax	*vs*. SMI_scoring	*vs*. DVT_echo
Acute						
DVT_Emean	≤14.50 kPa	0.96 (0.91–0.98)				
DVT_Emax	≤17.70 kPa	0.95 (0.89–0.97)	0.87			
SMI_scoring	≤1	0.93 (0.88–0.97)	0.39	0.44		
DVT_echo	≤ hypoecho	0.66 (0.57–0.74)	<0.001	<0.001	<0.001	
DVT_Emean + SMI_scoring	–	0.66 (0.58–0.75)	<0.001	<0.001	<0.001	0.98
Subacute						
DVT_Emean	≤19.76 kPa	0.54 (0.46–0.63)				
DVT_Emax	≤27.43 kPa	0.51 (0.42–0.60)	0.75			
SMI_scoring	≤2	0.53 (0.44–0.62)	0.73	0.84		
DVT_echo	≤ hypoecho	0.63 (0.54–0.71)	0.11	0.09	0.05	
DVT_Emean + SMI_scoring	–	0.90 (0.83–0.94)	<0.001	<0.001	<0.001	<0.001
Chronic						
DVT_Emean	>17.39 kPa	0.94 (0.88–0.97)				
DVT_Emax	>20.55 kPa	0.88 (0.81–0.93)	<0.001			
SMI_scoring	>2	0.91 (0.84–0.95)	0.31	0.53		
DVT_echo	≥ isoecho	0.76 (0.68–0.83)	0.014	0.01	0.002	
DVT_Emean + SMI_scoring	–	0.74 (0.66–0.82)	0.014	0.01	0.002	0.70

†, only AUCs were compared. ROC, receiver operating characteristic curve; DVT, deep vein thrombosis; AUC, area under the receiver operating characteristic curve; CI, confidential interval; DVT_Emean, the mean value of the elastic modulus for DVT; DVT_Emax, the maximum value of the elastic modulus for DVT; SMI_scoring, SMI's flow distribution scoring pattern; DVT_echo, deep vein thrombosis echogenicity; SMI, super microvascular imaging.

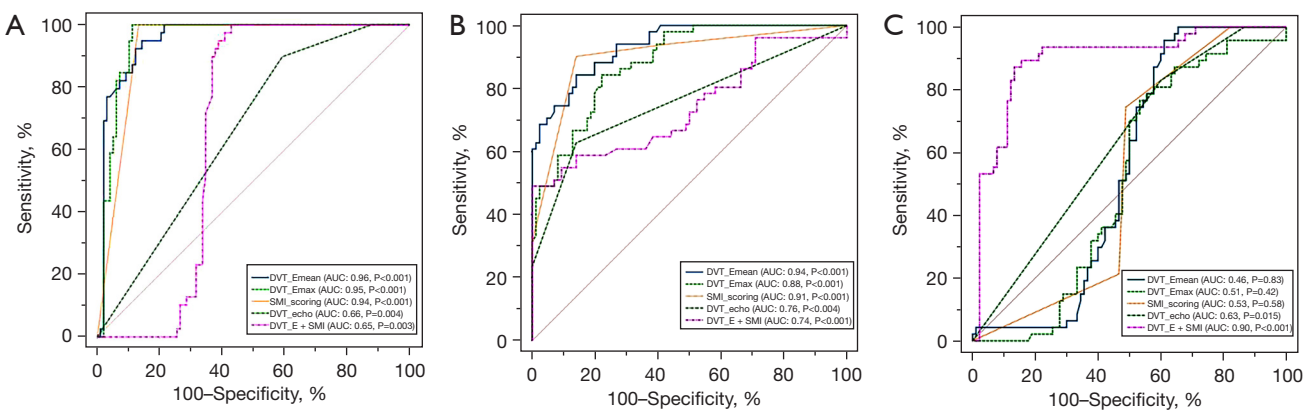

Figure 4 ROC curves of DVT_Emean, DVT_Emax, SMI_scoring, DVT_echo and the combined model in predicting DVT ages. (A) Acute (acute *vs*. subacute-chronic); (B) chronic (acute-subacute *vs*. chronic); (C) subacute (acute-chronic *vs*. subacute). Acute: ≤14 days; Subacute: 15–30 days; Chronic: 31 days to 6 months. DVT, deep venous thrombosis; DVT_Emean, the mean value of the elastic modulus for DVT; DVT_Emax, the maximum value of the elastic modulus for DVT; SMI_scoring, SMI's flow distribution scoring pattern; DVT_echo, deep vein thrombosis echogenicity; SMI, super microvascular imaging; AUC, area under the receiver operating characteristic curve; ROC, receiver operating characteristic.

Reproducibility test

There was excellent inter-observer agreement in the measurement of the following indices (intraclass correlation coefficient, 95% confidence interval): DVT_Emax (0.914, 0.823–0.959) and DVT_Emean (0.937, 0.869–0.972); SMI_scoring (0.887, 0.792–0.949) and DVT_echo (0.844, 0.698–0.923).

Discussion

The present study investigated the efficacy of using SMI and 2D-SWE to determine DVT age in patients with CT and BI. In patients with CT and BI, DVT_Emax and DVT_Emean reflected a progressive increase in thrombus stiffness over time. SMI_scoring, as a semi-quantitative indicator, also had good diagnostic value in staging by observing low-velocity blood gaps within thrombolysis and the formation of thrombotic neovascularization. However, none of these parameters showed significant efficacy in predicting subacute DVT. In addition, the combination of 2D-SWE and SMI did not improve the predictive value of acute and chronic DVT compared to 2D-SWE or SMI alone; however, their combination demonstrated significant effectiveness in predicting subacute DVT.

Studies have shown that catheter-directed thrombolysis may be the preferred primary approach for early stage DVT (less than 2 weeks of age) to protect valvular function after DVT, whereas mechanical thrombectomy may be more effective for older DVT (21-23). The 2020 American Society of Hematology Guidelines for the Treatment of Venous Thromboembolism emphasizes staged treatments for the therapeutic management of new DVT (1). So accurate determination of thrombus age is vital for guiding appropriate treatment decisions. However, relying on clinical symptoms for estimating disease onset is often imprecise, especially in the context of increased asymptomatic DVT detection rates due to the widespread use of US imaging (24). Despite its ability to detect asymptomatic DVT, traditional US has limitations when it comes to determining the age of thrombi, especially those less than two weeks old (13,25). This highlights the need for more effective diagnostic tools.

While other methods (e.g., nuclear medicine techniques and enhanced magnetic resonance venography) can satisfactorily determine thrombus age, they are not cost-effective and have limited accessibility (26,27). Previous studies have shown that 2D-SWE is the only effective and noninvasive method for both qualitative and quantitative evaluation of DVT elasticity (13,14,28); further, it is more objective and reproducible and allows for direct evaluation of tissue elasticity (11).

Our study established cutoff values of DVT_Emax (17.7, 20.6 kPa) and DVT_Emean (14.5, 17.3 kPa) for staging acute and chronic thrombus, which are consistent with those of previous studies, indicating high reproducibility (13,14,28). Nevertheless, the utility of thrombus echogenicity as a determinant of thrombus age is a subject of ongoing debate (25,28,29). While some researchers question the reliability of echogenicity as an age indicator (13,25), others have reported significant differences in echogenicity between acute and chronic thrombus groups (28,29).

Our results suggest that while DVT_echo does not reliably delineate the acute and subacute phases of DVT, it serves as a valuable tool for identifying chronic thrombophilic alterations, with AUC values ranging from 0.68 to 0.83. The inconsistency in findings may stem from varying criteria for thrombus age enrollment: some authors (28,29) consider thrombi to be chronic if they persist beyond eight months. During this extended period, thrombus fibrosis can result in scarring, wall thickening, and synechiae, potentially leading to partial, long-standing obstruction. The intraluminal residual material that exhibits heightened echogenicity is more accurately characterized as chronic post-thrombotic change rather than active thrombus (3,30,31). Additionally, the measurement of echogenicity is system-dependent and highly influenced by factors such as operator judgement, thrombus depth, transducer frequency, and grayscale US gain level. To mitigate measurement bias, we standardized the grayscale US settings for all participants. In light of our findings (*Table 4*), we construe hyperechoic thrombi as suggestive of chronic thrombosis. However, the presence of hypoechoic thrombi throughout the acute (90%), subacute (83%), and chronic (37%) stages hinders their effectiveness in differentiating among the various phases of thrombus formation.

SMI has been widely used to display microvascular flow in tumors of the parotid, breast, and other superficial organs and has offered substantial clinical benefits as documented in references (32-34). This investigation represents a pioneering effort to evaluate thrombus changes in human subjects by integrating 2D-SWE with SMI. Prior researches have verified the pathophysiological changes of thrombosis through animal experiments on rats, rabbits, large-body-weight pigs, and human specimens (35-39). They have

Table 4 Echogenicity of the thrombi and blood flow distribution according to SMI

DVT group	Echogenicity of the thrombus			Blood flow distribution according to SMI			
	Hypoechoic	Isoechoic	Hyperechoic	No flow within thrombus	Peripheral-arterial flow within thrombus	Flow area ≤50% thrombus	Flow area >50% thrombus
Acute (n=39)	35 [90]	4 [10]	0 [0]	39 [100]	0 [0]	0 [0]	0 [0]
Subacute (n=47)	39 [83]	8 [17]	0 [0]	10 [21]	25 [53]	12 [26]	0 [0]
Chronic (n=51)	19 [37]	20 [39]	12 [24]	3 [6]	2 [4]	30 [59]	16 [31]

Data are presented as number [percentage]. SMI, super microvascular imaging; DVT, deep vein thrombosis.

concluded that neovascularization can emerge in thrombosis within 3–7 days or over two weeks (the greater the weight, the later the onset of neovascularization), suggesting a similar evolutionary process in thrombus, which may be observed by SMI (35-39).

In our study, we observed that SMI possesses comparable diagnostic accuracy in both the acute and chronic thrombus phases to that of 2D-SWE (*Figure 4*). Although SMI was found to detect micro-arterial spectral Doppler signals in thrombi with or without intra-venous flow (53% of subacute cases), this individual indicator has little predictive value for the subacute phase. We propose two potential explanations for this finding. Firstly, the temporal sequence of endothelial arterialization of the venous wall may not align precisely with our current staging criteria. Secondly, while SMI adeptly visualizes the internal gaps of the thrombi's filling defect, the microarterial and venous flow images may sometimes overlap, leading to misinterpretation as changes indicative of the chronic phase. Consequently, we advocate for the integration of SMI with 2D-SWE to enhance diagnostic precision. And this combined approach really offered a more comprehensive assessment for subacute thrombus group than their alone (*Figure 4*).

H owever, it is important to note that the combination of 2D-SWE and SMI did not enhance the diagnostic efficacy for detecting DVT in the acute or chronic groups (*Figure 4*). This could be attributed to the fact that SWE already possesses high diagnostic accuracy as a standalone technique. Additionally, the misdiagnosis associated with SMI, as previously discussed, does not contribute to a significant improvement in diagnostic value. Furthermore, previous studies used conventional US and CDFI for 2D-SWE ROI placement, which could be inaccurate due to the inability to visualize very low-velocity flow signals and difficulty in differentiating their hypoechoic features from thrombi, leading to misidentified thrombus ROIs. In contrast, our study utilized SMI for the selection of 2D-SWE ROI, which may have yielded more precise 2D-SWE results by avoiding such pitfalls.

Clinical implications

Assessing thrombus age is essential for determining the appropriate treatment for DVT. Early detection and accurate evaluation of thrombus staging are crucial for preventing post-thrombotic syndrome, a condition that can significantly affect patients' quality of life and lead to serious complications, such as pulmonary embolism. Conventional US cannot effectively differentiate thrombus aging. In contrast, 2D-SWE can quantitatively evaluate thrombus stiffness and has been increasingly recognized for the assessment of acute and chronic thrombi. Additionally, SMI is capable of capturing the microfluidic changes that occur during venous thrombolysis. The combined application of SMI and 2D-SWE is quick and easy to perform and is a promising tool for evaluating thrombus age for clinicians in the future.

Study limitations

First, all 137 patients were hospitalized postoperatively and most received anticoagulation therapy; thus, it is possible that untreated thrombi behaved differently to treated thrombi. Second, ID-DVT was more common in postoperative patients with CT and BI than in those with CFVT/POPVT, and because of the application of anticoagulant drugs, our data showed that most cases of ID-DVT disappeared at chronic or earlier stages. Our study exclusively examined patients who developed DVT after CT or BI. Thus, assessments of thrombi caused by other factors and those located in the iliac and deep femoral vein regions were restricted. Third, this investigation was limited to our institution, underscoring the necessity to validate our

results in larger multicenter trials.

Conclusions

Thrombus staging is essential for making treatment decisions for DVT of the lower extremities. This study showed that 2D-SWE and SMI imaging techniques could be used to distinguish between the acute and chronic phases of DVT when such differentiation is necessary. SWE plus SMI is a promising adjunctive technique for determining the subacute phase of DVT. Monitoring thrombus stiffness and intra-thrombus neovascularization to reflect configuration changes in thrombi can assist clinicians in developing rational treatment strategies.

Acknowledgments

Funding: This research was funded by Tai'an Innovation Development Program for Science and Technology (Nos. 2021NS141 and 2021NS169).

Footnote

Reporting Checklist: The authors have completed the STARD reporting checklist. Available at https://qims.amegroups.com/article/view/10.21037/qims-23-1822/rc

Conflicts of Interest: All authors have completed the ICMJE uniform disclosure form (available at https://qims.amegroups.com/article/view/10.21037/qims-23-1822/coif). All authors report that this research was funded by Tai'an Innovation Development Program for Science and Technology (Nos. 2021NS141 and 2021NS169). The authors have no other conflicts of interest to declare.

Ethical Statement: The authors are accountable for all aspects of the work in ensuring that questions related to the accuracy or integrity of any part of the work are appropriately investigated and resolved. The study was conducted in accordance with the Declaration of Helsinki (as revised in 2013). The study was approved by the Institutional Review Board of The Second Affiliated Hospital of Shandong First Medical University (No. 202047) and informed consent was taken from all individual participants.

References

1. Ortel TL, Neumann I, Ageno W, Beyth R, Clark NP, Cuker A, et al. American Society of Hematology 2020 guidelines for management of venous thromboembolism: treatment of deep vein thrombosis and pulmonary embolism. Blood Adv 2020;4:4693-738.
2. Tovey C, Wyatt S. Diagnosis, investigation, and management of deep vein thrombosis. BMJ 2003;326:1180-4.
3. Needleman L, Cronan JJ, Lilly MP, Merli GJ, Adhikari S, Hertzberg BS, DeJong MR, Streiff MB, Meissner MH. Ultrasound for Lower Extremity Deep Venous Thrombosis: Multidisciplinary Recommendations From the Society of Radiologists in Ultrasound Consensus Conference. Circulation 2018;137:1505-15.
4. Fraser JD, Anderson DR. Deep venous thrombosis: recent advances and optimal investigation with US. Radiology 1999;211:9-24.
5. Wright DJ, Shepard AD, McPharlin M, Ernst CB. Pitfalls in lower extremity venous duplex scanning. J Vasc Surg 1990;11:675-9.
6. Robinson KS, Anderson DR, Gross M, Petrie D, Leighton R, Stanish W, Alexander D, Mitchell M, Mason W, Flemming B, Fairhurst-Vaughan M, Gent M. Accuracy of screening compression ultrasonography and clinical examination for the diagnosis of deep vein thrombosis after total hip or knee arthroplasty. Can J Surg 1998;41:368-73.
7. Clagett GP, Anderson FA Jr, Heit J, Levine MN, Wheeler HB. Prevention of venous thromboembolism. Chest 1995;108:312S-34S.
8. Kearon C, Akl EA, Ornelas J, Blaivas A, Jimenez D, Bounameaux H, Huisman M, King CS, Morris TA, Sood N, Stevens SM, Vintch JRE, Wells P, Woller SC, Moores L. Antithrombotic Therapy for VTE Disease: CHEST Guideline and Expert Panel Report. Chest 2016;149:315-52.
9. Bosio G, Zenati N, Destrempes F, Chayer B, Pernod G, Cloutier G. Shear Wave Elastography and Quantitative Ultrasound as Biomarkers to Characterize Deep Vein

Thrombosis In Vivo. J Ultrasound Med 2022;41:1807-16.
10. Durmaz F, Gultekin MA. Efficacy of Shear Wave Elastography in the Differentiation of Acute and Subacute Deep Venous Thrombosis. Ultrasound Q 2021;37:168-72.
11. Santini P, Esposto G, Ainora ME, Lupascu A, Gasbarrini A, Zocco MA, Pola R. Ultrasound Elastography to Assess Age of Deep Vein Thrombosis: A Systematic Review. Diagnostics (Basel) 2023;13:2075.
12. Mumoli N, Mastroiacovo D, Giorgi-Pierfranceschi M, Pesavento R, Mochi M, Cei M, Pomero F, Mazzone A, Vitale J, Ageno W, Dentali F. Ultrasound elastography is useful to distinguish acute and chronic deep vein thrombosis. J Thromb Haemost 2018;16:2482-91.
13. Pan FS, Tian WS, Luo J, Liu M, Liang JY, Xu M, Zheng YL, Xie XY. Added value of two-dimensional shear wave elastography to ultrasonography for staging common femoral vein thrombi. Med Ultrason 2017;19:51-8.
14. Hoang P, Wallace A, Sugi M, Fleck A, Pershad Y, Dahiya N, Albadawi H, Knuttinen G, Naidu S, Oklu R. Elastography techniques in the evaluation of deep vein thrombosis. Cardiovasc Diagn Ther 2017;7:S238-45.
15. Jiang ZZ, Huang YH, Shen HL, Liu XT. Clinical Applications of Superb Microvascular Imaging in the Liver, Breast, Thyroid, Skeletal Muscle, and Carotid Plaques. J Ultrasound Med 2019;38:2811-20.
16. Czaplicki C, Albadawi H, Partovi S, Gandhi RT, Quencer K, Deipolyi AR, Oklu R. Can thrombus age guide thrombolytic therapy? Cardiovasc Diagn Ther 2017;7:S186-96.
17. van Rij AM, Hill G, Krysa J, Dutton S, Dickson R, Christie R, Smillie J, Jiang P, Solomon C. Prospective study of natural history of deep vein thrombosis: early predictors of poor late outcomes. Ann Vasc Surg 2013;27:924-31.
18. Zheng J, Guo H, Zeng J, Huang Z, Zheng B, Ren J, Xu E, Li K, Zheng R. Two-dimensional shear-wave elastography and conventional US: the optimal evaluation of liver fibrosis and cirrhosis. Radiology 2015;275:290-300.
19. Ferraioli G, Tinelli C, Dal Bello B, Zicchetti M, Filice G, Filice C; Liver Fibrosis Study Group. Accuracy of real-time shear wave elastography for assessing liver fibrosis in chronic hepatitis C: a pilot study. Hepatology 2012;56:2125-33.
20. DeLong ER, DeLong DM, Clarke-Pearson DL. Comparing the areas under two or more correlated receiver operating characteristic curves: a nonparametric approach. Biometrics 1988;44:837-45.
21. Vedantham S, Sista AK, Klein SJ, Nayak L, Razavi MK, Kalva SP, Saad WE, Dariushnia SR, Caplin DM, Chao CP, Ganguli S, Walker TG, Nikolic B; Society of Interventional Radiology and Cardiovascular and Interventional Radiological Society of Europe Standards of Practice Committees. Quality improvement guidelines for the treatment of lower-extremity deep vein thrombosis with use of endovascular thrombus removal. J Vasc Interv Radiol 2014;25:1317-25.
22. Vedantham S, Grassi CJ, Ferral H, Patel NH, Thorpe PE, Antonacci VP, Janne d'Othée BM, Hofmann LV, Cardella JF, Kundu S, Lewis CA, Schwartzberg MS, Min RJ, Sacks D; Technology Assessment Committe of the Society of Interventional Radiology. Reporting standards for endovascular treatment of lower extremity deep vein thrombosis. J Vasc Interv Radiol 2006;17:417-34.
23. Vedantham S, Millward SF, Cardella JF, Hofmann LV, Razavi MK, Grassi CJ, Sacks D, Kinney TB. Society of Interventional Radiology position statement: treatment of acute iliofemoral deep vein thrombosis with use of adjunctive catheter-directed intrathrombus thrombolysis. J Vasc Interv Radiol 2009;20:S332-5.
24. Tini G, Moriconi A, Ministrini S, Zullo V, Venanzi E, Mondovecchio G, Campanella T, Marini E, Bianchi M, Carbone F, Pirro M, De Robertis E, Pasqualini L. Ultrasound screening for asymptomatic deep vein thrombosis in critically ill patients: a pilot trial. Intern Emerg Med 2022;17:2269-77.
25. Murphy TP, Cronan JJ. Evolution of deep venous thrombosis: a prospective evaluation with US. Radiology 1990;177:543-8.
26. Froehlich JB, Prince MR, Greenfield LJ, Downing LJ, Shah NL, Wakefield TW. "Bull's-eye" sign on gadolinium-enhanced magnetic resonance venography determines thrombus presence and age: a preliminary study. J Vasc Surg 1997;26:809-16.
27. Brighton T, Janssen J, Butler SP. Aging of acute deep vein thrombosis measured by radiolabeled 99mTc-rt-PA. J Nucl Med 2007;48:873-8.
28. Rubin JM, Xie H, Kim K, Weitzel WF, Emelianov SY, Aglyamov SR, Wakefield TW, Urquhart AG, O'Donnell M. Sonographic elasticity imaging of acute and chronic deep venous thrombosis in humans. J Ultrasound Med 2006;25:1179-86.
29. Fowlkes JB, Strieter RM, Downing LJ, Brown SL, Saluja A, Salles-Cunha S, Kadell AM, Wrobleski SK, Wakefield TW. Ultrasound echogenicity in experimental venous thrombosis. Ultrasound Med Biol 1998;24:1175-82.
30. Markel A. Origin and natural history of deep vein thrombosis of the legs. Semin Vasc Med 2005;5:65-74.

31. Comerota AJ, Oostra C, Fayad Z, Gunning W, Henke P, Luke C, Lynn A, Lurie F. A histological and functional description of the tissue causing chronic postthrombotic venous obstruction. Thromb Res 2015;135:882-7.
32. Zhao L, Mu J, Mao Y, Xin X. Diagnostic Value of Superb Microvascular Imaging in Parotid Tumors. Med Sci Monit 2020;26:e921813.
33. Zhu Y, Tang Y, Zhang G, Zhang J, Li Y, Jiang Z. Quantitative analysis of superb microvascular imaging for monitoring tumor response to chemoradiotherapy in locally advanced cervical cancer. Front Oncol 2022;12:1074173.
34. Zhu YC, Zhang Y, Deng SH, Jiang Q. Diagnostic Performance of Superb Microvascular Imaging (SMI) Combined with Shear-Wave Elastography in Evaluating Breast Lesions. Med Sci Monit 2018;24:5935-42.
35. Turpie AG, Chin BS, Lip GY. Venous thromboembolism: pathophysiology, clinical features, and prevention. BMJ 2002;325:887-90.
36. Line BR. Pathophysiology and diagnosis of deep venous thrombosis. Semin Nucl Med 2001;31:90-101.
37. Diaz JA, Obi AT, Myers DD Jr, Wrobleski SK, Henke PK, Mackman N, Wakefield TW. Critical review of mouse models of venous thrombosis. Arterioscler Thromb Vasc Biol 2012;32:556-62.
38. Hendley SA, Dimov A, Bhargava A, Snoddy E, Mansour D, Afifi RO, Wool GD, Zha Y, Sammet S, Lu ZF, Ahmed O, Paul JD, Bader KB. Assessment of histological characteristics, imaging markers, and rt-PA susceptibility of ex vivo venous thrombi. Sci Rep 2021;11:22805.
39. Yuriditsky E, Narula N, Jacobowitz GR, Moreira AL, Maldonado TS, Horowitz JM, Sadek M, Barfield ME, Rockman CB, Garg K. Histologic assessment of lower extremity deep vein thrombus from patients undergoing percutaneous mechanical thrombectomy. J Vasc Surg Venous Lymphat Disord 2022;10:18-25.

Cite this article as: Peng L, Liu Y, Lv C, Shen W, Wu Y, Zhang J, Fu Z. Evaluating the stage of deep vein thrombosis: the diagnostic accuracy of shear wave elastography and super-microvascular imaging. Quant Imaging Med Surg 2024. doi: 10.21037/qims-23-1822